Critical properties of non-equilibrium crumpled systems

1992 J. Phys. A: Math. Gen. 25 L353

(http://iopscience.iop.org/0305-4470/25/7/012)

J. Phys. A: Math. Gen. 25 (1992) L353–L357. Printed in the UK

LETTER TO THE EDITOR

Critical properties of non-equilibrium crumpled systems

J B C Garcia, M A F Gomes, T I Jyh and T I Ren

Departamento de Física, Universidade Federal de Pernambuco, 50739 Recife, Pernambuco, Brazil

Received 25 October 1991

Abstract. Geometrical and statistical properties of non-equilibrium crumpled surfaces (CS) and crumpled wires (CW) are investigated and compared. The relationship between the geodesic distance x and the Pythagorean distance r in CS and CW and their dependence on the linear (uncrumpled) size L is studied. Among other results we show that the moments of the probability distribution $P(x, r)$ for CS requires an infinite hierarchy of critical exponents.

The statistical physics and the geometric properties of crumpled manifolds (CM) is at present a subject of wide interest. Besides their intrinsic interest, the study of CM has connections with a number of areas varying from polymer, membrane and interface physics to gauge theories. The literature on CM concerns to a great extent the properties of self-avoiding model manifolds at equilibrium [1]. This letter deals, in contrast, with the statistical physics and the geometric properties of non-equilibrium CM (NECM).

Geometrical and physical properties of NECM obtained from random and irreversible compactification of paper sheets, aluminium foils and metallic threads have been recently studied [2–4] and we refer to [3] for additional insight into the topic. The non-equilibrium behaviour of crumpled surfaces (CS) [2, 3] and crumpled wires (CW) [4] is analysed here in further detail, and new critical phenomena associated with these systems are discussed. A schematic classification of non-equilibrium crumpling processes is also suggested in the sixth paragraph. The results presented in this letter are based on experimental measurements obtained from large ensembles of CS and CW with approximately one thousand objects. The experimental procedures are similar to those discussed in the first paragraphs of the recent references [3, 4].

In [3] we studied how the three-dimensional 'air' or Pythagorean distance $r(Q, Q')$ between two points Q and Q' on a CS transforms into the internal or geodesic distance $x(Q, Q')$, with probability $P(x, r)$, after the unfolding of the CS on a plane. Among other results, we found in [3] that the average of x, $\langle x\rangle$, scales as $\langle x\rangle \sim r^{1/3}$, for a fixed linear (uncrumpled) size L of the CS. Here we present new scaling relations based on an extension of the experimental procedure used in [3]. Then, instead of considering a single value of L as in [3], we work in this letter with different values of the size L. Firstly, we have obtained that $\langle x\rangle \sim L^{0.69\pm0.05}$, $5\ \mathrm{cm} \leqslant L \leqslant 66\ \mathrm{cm}$, irrespective of r. Equivalently we can write $\langle x\rangle \sim R^{0.86\pm0.06}$, where $R \sim L^{0.8}$ is the average radius of the CS [3]. Thus, if we consider the dependences of $\langle x\rangle$ on both r and L (or R) we obtain

$$\langle x\rangle(\mathrm{CS}) \sim r^{1/3}L^{0.69} \sim r^{1/3}R^{0.86}. \tag{1}$$

By definition the Pythagorean and the internal (geodesic) distances in CM satisfy $r < \langle x\rangle$. In principle, it is natural to suppose that $\langle x\rangle \sim r^{\alpha}R^{\beta}$ and thus $\langle x\rangle(r = R) \sim r^{\alpha+\beta} > r$

leads to $\alpha+\beta>1$, or $\beta>1-\alpha=\frac{2}{3}$ for CS, as shown in (1). Secondly, the standard deviation σ_x of x with respect to the average $\langle x\rangle$ has a strong dependence on L, and scales as $\sigma_x \sim L^{1.22\pm0.02}$ with a coefficient of correlation of 0.99 irrespective of r. Thus, the relative fluctuations $\sigma_x/\langle x\rangle$ diverges for r fixed as $L^{0.53\pm0.07}$ ($R^{0.66\pm0.09}$) as $L(R)$ goes to the infinity. Thirdly, the binned probability distribution $P(x,r)$ for CS can be approximated by the power law $P_0(x,r)\sim x^{-\xi}$, with $\xi=1.4\pm0.3$ provided $r<R$. This fit does not depend on L, nor on the number of bins used to analyse the distribution.

For crumpled balls made of wires with distinct compositions of lead and tin, and lengths L in the interval $1\ \mathrm{m}\leqslant L\leqslant 10\ \mathrm{m}$, we have now obtained the following scaling relations involving the geodesic and the Pythagorean distances.

(i) $\langle x\rangle \sim r^{-0.02\pm0.03}$, irrespective of L; i.e. $\langle x\rangle$ is independent of $r(r>0)$ (or possibly has a logarithmic dependence on r), for L fixed in the interval considered.

(ii) $\langle x\rangle\sim L^{1.01\pm0.06}$, for r fixed in the interval $0.05\leqslant r/2R\leqslant 1$. R is the average radius of the CW. Using the scaling $L\sim R^{2.75}$ valid for CW [4] we can analogously write $\langle x\rangle\sim R^{2.78\pm0.17}$. If we consider the dependences of $\langle x\rangle$ on r and L we may write in correspondence with (1)

$$\langle x\rangle(\mathrm{CW})\sim r^0L^1\sim r^0R^{2.75}. \qquad (2)$$

(iii) The standard deviation σ_x of x with respect to the average $\langle x\rangle$ is also independent of r; it behaves as $\sigma_x\sim r^{0.01\pm0.04}$.

(iv) The minimum x, $x_{\min}$, in a series of a hundred values of the geodesic length (with L fixed) depends on r. More precisely, we observed that $x_{\min}\sim r^{d_{\min}}$, with $d_{\min}=-0.15\pm0.17$.

(v) The binned probability distribution $P(x,r)$ for CW can be approximated by the power law $P_0\sim x^{-\xi}$, with $\xi=0.75\pm0.25$, irrespective of $r<R$, L, and the number of bins used to analyse the distribution.

It is interesting to compare the hierarchy of behaviours of the average geodesic distance versus the Pythagorean distance for CS, CW, and other mathematical structures. For a smooth spherical surface, for example, $\langle x\rangle$ is trivially given by the concave function $\langle x\rangle=2R\sin^{-1}(r/2R)$, where R is the radius of the sphere (curve *a* in figure 1). Differently, for CS (with the linear size L or the average radius R fixed) $\langle x\rangle$ is given by the convex function $\langle x\rangle\sim r^{1/3}$ as shown in figure 1, curve *b*. For a CW, $\langle x\rangle$ is independent of r (or presents a logarithmic dependence on r) as shown in figure 1, curve *c*. These three categories of behaviour for $\langle x\rangle(r)$ are limited from below by the straight line $\langle x\rangle=r$ (dashed line in figure 1) corresponding to the plane geometry or the flat state, and from above by the line $\langle x\rangle(r>0)=\infty$ (dotted line in figure 1) corresponding to any mathematical fractal.

As discussed in the third and fourth paragraphs, the binned probability distribution $P(x,r)$ for CS and CW can be described approximately by $P_0\sim x^{-\xi}$, irrespective of $r<R$, L, and the number of bins. If we consider this approximation, we obtain for the average geodesic distance in CS and CW:

$$\langle x\rangle=\int_r^{aL}P_0(x,r)x\,\mathrm{d}x\bigg/\int_r^{aL}P_0(x,r)\,\mathrm{d}x=\frac{-\xi+1}{-\xi+2}\,\frac{(aL)^{-\xi+2}-r^{-\xi+2}}{(aL)^{-\xi+1}-r^{-\xi+1}} \qquad (3)$$

where $\xi\neq1$ and r is fixed ($r<R$). In (3) $a=\sqrt{2}$ for CS and $a=1$ for CW. There are three important cases to be considered in connection with (3): (i) for $\xi<1$, and $L\gg r$, we have $\langle x\rangle\sim r^0L^1$; this is the behaviour observed for CW (fourth paragraph). (ii) If $1<\xi<2$, $L\gg r$, we obtain $\langle x\rangle\sim r^{\xi-1}L^{-\xi+2}$. If $\xi=\frac{4}{3}$ we get $\langle x\rangle\sim r^{1/3}L^{2/3}$; this is the same as (1) which describes the behaviour of $\langle x\rangle$ as a function of r and L for CS. (iii) Finally,

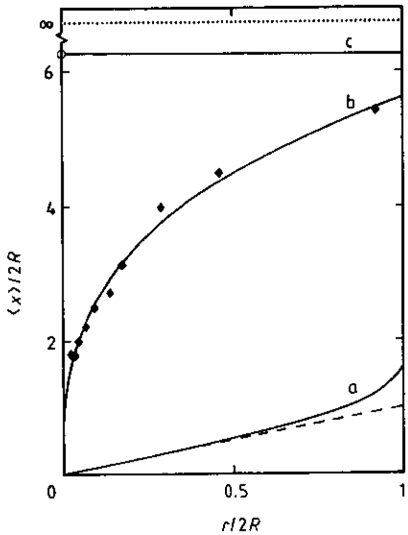

Figure 1. The dependence of the average geodesic distance $\langle x\rangle$ on the Pythagorean distance r for spherical surfaces (a), crumpled surfaces (b), and crumpled wires (c). R is the radius of the sphere in (a) and the ensemble average radius in (b). Dashed and dotted lines represent the behaviour of $\langle x\rangle(r)$ for the flat state ($\langle x\rangle = r$), and for the mathematical fractals ($\langle x\rangle = 0$, for $r = 0$, and $\langle x\rangle = \infty$ $\forall r > 0$) respectively. ● denotes experimental data.

for $\xi > 2$, $L \gg r$, we have $\langle x\rangle \sim r^1 L^0$, which describes the flat phase. Thus, in general we have $\langle x\rangle \sim r^\alpha L^\gamma$, with $\alpha + \gamma = 1$, $r \ll L$. Within the approximation considered in this paragraph, the dependence of the exponents α and γ as a function of the exponent ξ suggests the classification of the crumpling processes shown in figure 2.

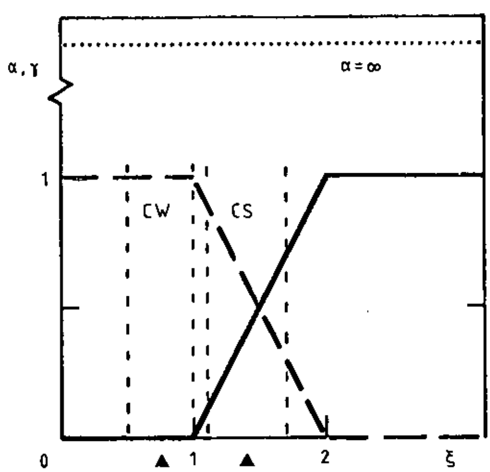

Figure 2. The dependence of the critical exponents α (continuous line) and γ (dashed line) on the exponent ξ for the approximation discussed in the sixth paragraph. The dotted line refers to the value $\alpha = \infty$ associated with the mathematical fractals. Triangles (▲) and vertical dashed lines designate respectively the average ξ and the interval of variability of ξ for CW and CS (experimental data).

In order to obtain a more detailed understanding of the crumpling processes in surfaces we calculated the moments

$$M_k(r)=\sum_x P(x, r)x^k \tag{4}$$

using the (binned) experimental distribution $P(x, r)$ that connects the Pythagorean (r) and the geodesic (x) distances in CS. We have observed that different moments M_k scale as different power laws $M_k \sim r^{\delta_k}$, where the critical exponents δ_k are given by the continuous line shown in figure 3. We note in passing that if we approximate the experimental $P(x, r)$ in (4) by the power law $P_0 \sim x^{-\xi}$, $\xi=1.4$, as mentioned in the third paragraph, we obtain $M_k \to M_{0k} \sim r^{\delta_{0k}}$, with $\delta_{0k}=-\xi+k+1=-0.4+k$, for $k<\xi-1=0.4$, and $\delta_{0k}=0$, for $k>\xi-1=0.4$. This approximation for the δ_k is shown in figure 3 (dotted lines). The dashed line in figure 3 refers to a better approximation to the exponents δ_k. It is obtained after the substitution

$$P(x, r) \to P'(x, r)=A\frac{r^\alpha}{(x-r)^{1+\alpha}}\exp\left(\frac{-Br^\alpha}{(x-r)}\right) \tag{5}$$

with $\alpha=\frac{1}{4}$, $B=0.055$, in (5). This distribution function satisfies $P' \to 0$ for $x \to r$, and $P' \sim x^{-5/4}$, for large x and small r. Both conditions are observed by the experimental distribution $P(x, r)$ within the statistical uncertainties. Equation (5) is a good approximation to $P(x, r)$, if $r<R$. This is confirmed in figure 4 where we exhibit the best fits (5) to the experimental distribution $P(x, r)$ for $r/L=\frac{1}{330}$; $\frac{1}{220}$; $\frac{1}{165}$; $\frac{1}{110}$ and $\frac{2}{165}$. The average radius of the ensemble of CS in this case satisfies $R/L=0.0654$. All the fitted data collapse on a single curve of the form (5) with $B=0.055 \pm 0.001$ irrespective of r.

The general subject discussed in this letter has been the scaling properties of non-equilibrium crumpled systems with the topology of the line (CW) and of the plane (CS). The statistical physics of these systems is complex and not well understood. Thus, for example, it is not clear if the diffusion-limited growing self-avoiding surfaces

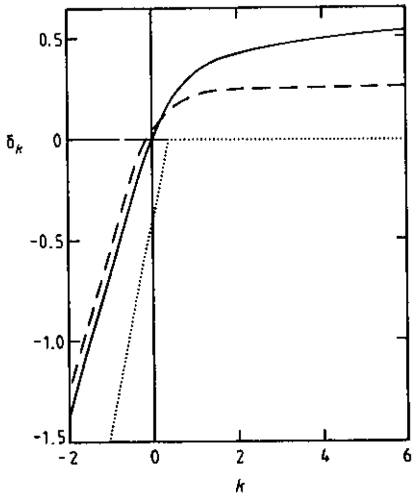

Figure 3. The critical exponents δ_k associated with the scaling relations $M_k \sim r^{\delta_k}$, where M_k are the moments defined in (4). Continuous, dashed, and dotted lines refer respectively to M_k obtained with the experimental $P(x, r)$, with the approximation (5), and with the approximation $P \to P_0 \sim x^{-\xi}$.

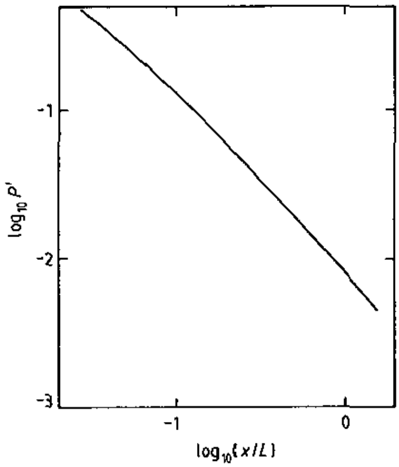

Figure 4. The best fit to the experimental distribution $P(x, r)$ using the distribution $P'(x, r)$ given in (5) for different values of the Pythagorean distance r. The $P'(x)$ for different values of r collapse on the single curve shown in the figure.

(DLSAS) of Debierre and Bradley [5] present the critical properties of CS discussed here. DLSAS and CS have the same fractal dimension within the statistical uncertainties. CW and CS are new paradigms of disordered systems. They are also an experimental manifestation of ill-condensed matter and self-organized criticality [6]. It is interesting to observe that CS have a kind of complementary relationship with Plateau's problem [7], one of the deeper problems of the calculus of variations. Both problems refer to a surface S with area A bounded by a contour C. In Plateau's problem C is fixed and A varies, while in CS A is fixed and C varies. We hope that the results presented in this letter will lead to further investigations into the physics of non-equilibrium crumpled systems.

This work was partially supported by Conselho Nacional de Desenvolvimento Científico e Tecnológico and Financiadora de Estudos e Projetos of Brazil.

References

[1] Kantor Y, Kardar M and Nelson D R 1987 *Phys. Rev.* A **35** 3056
Plischke M and Boal D 1988 *Phys. Rev.* A **38** 4943
Hwa T 1990 *Phys. Rev.* A **41** 1751
Machta J and Kirkpatrick T R 1990 *Phys. Rev.* A **41** 5345
Plischke M and Fourcade B 1991 *Phys. Rev.* A **43** 2056
[2] Gomes M A F and Vasconcelos G L 1988 *Phys. Rev. Lett.* **60** 237
Gomes M A F, Jyh T I, Ren T I, Rodrigues I M and Furtado C B S 1989 *J. Phys. D: Appl. Phys.* **22** 1217
[3] Gomes M A F, Jyh T I and Ren T I 1990 *J. Phys. A: Math. Gen.* **23** L1281
[4] Albino Aguiar J, Gomes M A F and Neto A S 1991 *J. Phys. A: Math. Gen.* **24** L109
[5] Debierre J M and Bradley R M 1989 *J. Phys. A: Math. Gen.* **22** L213
[6] Gomes M A F, Lima F F and Oliveira V M 1991 *Phil. Mag. Lett.* in press
[7] Courant R 1940 *Am. Math. Monthly* **XLVII** 167